

Document downloaded from:

<http://hdl.handle.net/10251/117876>

This paper must be cited as:

Sarmiento, PA.; Torres Górriz, B.; Ruiz, DM.; Alvarado Vargas, YA.; Gasch, I.; Machuca, AF. (2019). Cyclic behavior of ultra-high performance fiber reinforced concrete beam-column joint. *Structural Concrete*. 20(1):348-360. <https://doi.org/10.1002/suco.201800025>



The final publication is available at

<https://doi.org/10.1002/suco.201800025>

Copyright John Wiley & Sons

Additional Information

Cyclic behavior of UHPFRC beam-column joint.

Cyclic loading in UHPFRC.

Patricia A. Sarmiento¹; Benjamín Torres^{2*}; Daniel M. Ruiz³; Yezid A.

Alvarado⁴; Isabel Gasch⁵ Andrés F. Machuca⁶

¹ Student, Pontificia Universidad Javeriana. Calle 40 # 5-50 Ed. José Gabriel Maldonado, Bogotá, Colombia. E-mail: patriciasarmiento@javeriana.edu.co

^{2*} Lecturer, ICITECH, Universitat Politècnica de València. Camino de Vera s/n, 46022 Valencia, Spain. Telephone number: +34 96 387 70 00 (Ext:76726) E-mail: bentorgo@upvnet.upv.es (Corresponding author)

³ Lecturer, Pontificia Universidad Javeriana. Calle 40 # 5-50 Ed. José Gabriel Maldonado, Bogotá, Colombia. E-mail: daniel.ruiz@javeriana.edu.co

⁴ Lecturer, Pontificia Universidad Javeriana. Calle 40 # 5-50 Ed. José Gabriel Maldonado, Bogotá, Colombia. E-mail: alvarado.y@javeriana.edu.co

⁵ Lecturer, IDM, Universitat Politècnica de València. Camino de Vera s/n, 46022 Valencia, Spain. Telephone number: +34 96 387 70 00 (Ext:76726) E-mail: igasch@upv.es

⁶ Student, Pontificia Universidad Javeriana. Calle 40 # 5-50 Ed. José Gabriel Maldonado, Bogotá, Colombia. E-mail: andres_machuk88@hotmail.com

Abstract

Ultra-high performance fiber reinforced concrete (UHPFRC) is a unique class of fiber-reinforced concrete featuring ultra-high compressive strength and ductile tensile strain hardening behaviour, accompanied by multiple narrow cracking. Although many studies have confirmed its superior mechanical and damage tolerance properties under monotonic or blast loading, limited research has been carried out on the cyclic performance of UHPFRC structural members. This paper proposes the use of UHPFRC to improve the cyclic performance of structural elements. An experimental program was carried out on a large number of UHPFRC beam-column joint specimens under a cyclic lateral load. After the cyclic loading test, the following results were obtained: 1) hysterical performance, 2) maximum load, 3) maximum displacement, 4) the maximum energy dissipation (measured by hysteresis cycles), 5) stiffness degradation 6) the cracking pattern and 6) the cracking area. The analysis showed that UHPFRC specimens have at least 157% higher energy dissipation than non fiber conventional reinforced concrete (RC). The initial stiffness of UHPFRC specimens without fibers (NF) was at least 23% higher than the RC specimen. For UHPFRC with fiber, initial stiffness was at least 45% higher than RC specimen.

Keywords: Ultra High Performance Fiber Reinforced Concrete, UHPFRC, energy dissipation capacity, cyclic lateral load, hysteresis load cycles, pattern cracking, stiffness degradation.

1. Introduction.

Seismic actions often end with desolate landscapes, the loss of human lives and damage or destruction of infrastructures [1].

Some of the most dramatic of these events have occurred in Indonesia and Italy in 2009, Japan, Turkey and Spain in 2011, the Philippines, Iran, Pakistan and China in 2013, and more recently, Nepal and Italy in 2015 and 2016, respectively. For example, the city of Lorca (Spain), suffered an earthquake of magnitude $M_w = 5.1$ in 2011[2], when many buildings were severely damaged. The movements generated by the earthquake, together with the special characteristics of the reinforced concrete building structures in the region, gave rise to different types of structural damage, killing nine persons and injuring 324. Most of the buildings in the city had reinforced concrete structures, which, due to their design combined with the severity of the earth tremors, were at serious risk of collapse. In fact, many had to be subsequently demolished and others needed retrofitting [2].

An ever growing number of books and papers are published each year on the subject [3–6] and a number of research groups [7–14] have studied the most frequent causes of the failure of reinforced concrete structures under seismic loads. The principal cause of building collapse is critical damage to columns and beam-column joints [15–17].

In order to ensure that reinforced concrete structures show good behaviour under seismic loads, the structural components must have a certain degree of ductility [17]. At the present time reinforced concrete (RC) structures are often built in seismic zones without complying with the required minimum building standards and thus need to be strengthened to be able to survive a seismic event without suffering serious damage. The structural elements in existing conventional RC buildings are thus frequently strengthened to improve their seismic behavior by increasing their ductility and energy dissipation capacity [14,17–23]. However, technological advances have produced new structural materials such as Ultra-high performance fiber reinforced concrete (UHPFRC), which has been the subject of many studies in recent years.

UHPFRC consists of high-strength cementitious materials, steel fibers, ground quartz, and super plasticizer [24–26]. UHPFRC has less permeability, creep and shrinkage than conventional concrete [27], while it also features compressive strengths above 150 MPa, elastic moduli over 46 GPa, usable tensile strengths in excess of 5 MPa, and high damage tolerance [28,29]. Its behaviour under tensile stresses allows the reinforcement to be totally or partially replaced, reducing construction times and improving structural properties. Its service life is longer than conventional concrete thanks to its lower water/cement ratio, which also improves its waterproofing qualities.

Many studies have confirmed the superior mechanical and damage tolerance properties of UHPFRC under monotonic or blast loading. According to [30] there are published studies where the direct tensile and the flexural behaviors of UHPFRC have been investigated and the superior tensile strength and post-crack energy absorption have been highlighted. There are also studies on the performance of UHPFRC (material) under cyclic loading (reference [30]), and it is evident that the structural elements is highly affected by the behavior of the UHPFRC. According to [30] there is a degradation of the modulus of elasticity of the UHPFRC with the number of loading cycles. The results of [30] indicated that the modulus of elasticity was considerably reduced after the first loading cycle, and then it was slightly

further reduced as the number of loading cycles was increased. However, limited research has been carried out on the cyclic performance of UHPFRC structural members [31], since the first publications on testing UHPFRC members under cyclic loads date from 2004 [32,33]. The appealing mechanical performance of UHPFRC has motivated researchers and engineers to evaluate their application in earthquake-resistant structures [34–40].

The seismic behavior of UHPFRC columns depends on the axial load level, stirrup arrangement and the fibers content. In the references [41-43] tested a lot of specimens of UHPFRC subjected to axial loads (columns). According to the results UHPFRC columns with multiple stirrups and commonly used structural steel ratios demonstrated excellent seismic behavior. Hosinieh et al. [42] demonstrated that a UHPFRC column could develop excellent displacement ductility capacity when it has closely-spaced and well-detailed transverse reinforcement (transverse reinforcement confining the cross section). Also the tests indicate that spacing and configuration of transverse reinforcement are important factors affecting the toughness of UHPFRC columns (area under the load–strain curve improves increasing the transverse reinforcement) and the configuration of the transverse reinforcement does not have a significant effect on column axial strength. As in conventional reinforced concrete columns, the axial load has a negative effect on the curvature ductility capacity of a UHPFRC column (the higher the axial load, the lower the curvature ductility capacity of the cross section). In [43], pure axial load tests showed a pronounced effect of the volumetric ratio of the transverse reinforcement on the confinement; and the authors of [44] concluded that the steel fibers of the UHPFRC columns controlled brittle cover spalling very well and assisted the transverse confinement reinforcement after the peak load. However, and according to [45], in a frame a UHPFRC column could maintain its strength at higher inter-story drifts ratios than a conventional reinforced concrete column. That is because the axial load ratio ($\text{Ultimate Load} / (\text{Gross area}) * (\text{compression strength})$) for the conventional reinforced concrete column was higher than the ratio for the UHPFRC column due to the high compressive strength of the UHPFRC. According to this, if a reinforced concrete column is compared with a UHPFRC column (both with the same axial load), the smaller axial load ratio of UHPFRC column compared with the conventional concrete column minimize the axial load effect at the post-elastic stage (bending) in the UHPFRC structure.

In this context, the study described in this paper assessed the feasibility of using UHPFRC to improve the seismic performance of structural elements by means of an experimental program on a large number of

UHPFRC beam-column joint specimens with various dosages of steel fibers and one reference reinforced concrete specimen, tested under cyclic lateral load.

UHPFRC is internally reinforced by 13 mm long straight steel fibers (SF) and 60 mm long hooked steel fibers (HF) at different dosages per volume of concrete (0%, 0.5%, 1%, 1.5%, 2% for HF and 1.5% for SF). The specimen design was based on NSR-10 [40] with moderate energy dissipation capacity (DMO). The main objective of the study was to determine the behaviour of UHPFRC specimens under cyclic loads, including: 1) maximum energy dissipation (measured by hysteresis cycles), 2) stiffness degradation, 3) hysterical performance, 4) maximum load, 5) maximum displacement, 6) the cracking pattern and 6) the cracking area.

2. Experimental program.

In order to characterise its behaviour against cyclic loads, a total of 11 specimens were built with the geometry and characteristics shown in Figure 1a and Table 1. The columns of specimens to be tested were 1.3 m long with a 0.2 m square cross section (minimum dimensions of a structural element with moderate energy dissipation MDO according to NSR-10) [40]. The longitudinal reinforcement was four 12 mm round rebars with 150 x 150 mm stirrups 10 mm in diameter. The concrete cover was 25 mm thick. The compressive strength f'_c of the concrete used in the specimens and the number of specimens tested are given in Table 1. All the specimens had the same geometry and reinforcement, and only differed in the fibers dosage per concrete volume.

Table 1. Specimen test of the experimental test.

Specimen	% Fiber	Type of fiber	Cross section (mmxmm)	f'_c (MPa)	Number of specimens	Diameter steel reinforcement (mm)		
						Long.	Stirrup	
RC	0	-	200x200	21	1	4 Φ 12	10	
NF	0	-	200x200	141	1	4 Φ 12	10	
UHPFRC	0.5%	0.5	200x200	125	2 (A, B)	4 Φ 12	10	
	1%	1	200x200	146	2 (A, B)	4 Φ 12	10	
	1.5%	1.5	200x200	147	2 (A, B)	4 Φ 12	10	
	2%	2	200x200	154	1	4 Φ 12	10	
	1.5% SF	1.5	Straight fiber SF	200x200	129	2 (A, B)	4 Φ 12	10
			Hooked Fiber HF					

The concrete is internally reinforced by 13 mm long straight steel fibers (SF) and 60 mm hooked steel fibers (HF) included at different dosages by volume of concrete. The approximate mixture composition

used throughout the study is shown in Table 2. The effect of fiber reinforcement on the compressive properties of this concrete was not studied.

Table 2. Mix proportions of UHPFRC

	Type of mix. UHPFRC					
	0%	0.5%	1%	1.5%	2%	1.5%
	NF	HF	HF	HF	HF	SF
Cement	1	1	1	1	1	1
Fine sand	0.96	0.94	0.93	0.91	0.89	0.91
Silica fume (S.F.)	0.2	0.2	0.2	0.2	0.2	0.2
Calcium carbonate (C.C.)	0.3	0.3	0.3	0.3	0.3	0.3
Steel fibers	0	0.5	1	1.5	2	1.5
High-range water-reducing admixture	0.027	0.027	0.027	0.027	0.027	0.027

The beam of each specimen were placed on a footing with reinforcement similar to the column reinforcement, simulating a column-beam joint. This element was anchored to the horizontal reaction slab by metal ties.

Four tubular steel beams tied the footing to the strong reaction frame using 4 threaded rods which were also tied to the bottom steel reaction frame through 2 tubular steel beams (Figure 1b). This system ensured that the footing base would not move or turn.

All specimens were tested at an age of 28 days. The curing of the specimens was done by spraying water twice a day for the first 7 days.

Each specimen was subjected to a reverse cyclic lateral load in displacement control. Controlled cyclic (sinusoidal) displacements were applied to the upper part of the columns, as shown in Figure 2. The displacements were small at first, until reaching drift ratio levels close to 6% of the column's length. Three full cycles of reverse lateral loading were applied in each run. Each specimen was loaded until either a load drop of approximately 6% of the drift ratio or irreparable damage occurred.

Each specimen was tested individually. Figure 3 shows the set-up of the specimens in the laboratory test. The displacement of the footing in the horizontal plane was measured by an LVDT system to guarantee the correct anchorage. To control the stability of the test during the loading cycles three LVDTs were fitted to the column at the base, middle-section and top.

In addition, monotonic test were made on the material. Bending test were made on three specimens according to ASTM C78-10. Figure 4 show the results and the degradation of the mechanical properties for high levels of strain can be seen.

3. Analysis procedure.

After the specimens had been tested the load-displacement hysteresis curves were drawn. The ductility of each specimen was obtained from the hysteresis curves, considering the maximum displacement reached. The energy dissipation capacity was obtained by the area of the trapezoids for each load-displacement cycle, as recommended in [41], which was designed for non-linear static methodologies. The hysteretic performance of each specimen was evaluated from the energy dissipated. Stiffness variations of each specimen was obtained as the ratio between the load applied and displacement.

4. Results and discussion.

This section reports on the general results of the experimental program. It indicates the differences between the tests with different fiber dosages, the comparison between the specimen responses, energy dissipation capacity, stiffness degradation, the influence of the cracking pattern and the main specimen failure modes.

4.1. Hysteretic response: Load-displacement results.

The behaviour of the specimens was evaluated by the relationship between the displacements applied to the upper part of the columns and the loads obtained. The graphs in Figure 5 a-k give the hysteresis cycles for all the specimens up to a drift ratio of 6% (displacement of 78 mm), although some tests reached 8% (displacement of 104 mm).

The similarity of the results obtained for each pair of specimens should be pointed out here (Graphs a-b, c-d, e-f, g-h) as well as the resulting symmetry of both displacement directions.

Figure 5 (j) and (k) show similar maximum load values for the NF and RC specimen, clearly lower than the loads reached by the UHPFRC specimens with fibers. On average, the maximum load reached by the UHPFRC specimens with fiber dosages is 30% higher than that of the NF specimen, and a 47% higher than that of the RC specimen.

From these figures, it can be seen that adding fibers clearly increases the energy dissipation capacity. It can be seen that the UHPFRC specimens have a larger area inside the hysteric cycle than the RC and NF specimens, showing the formers' greater energy dissipation capacity. It should be noted the similarity of the results obtained for each pair of specimens (0.5%-A and 0.5%-B; 1%-A and 1%-B; 1.5%-A and 1.5%-B; 1.5%SF-A and 1.5%SF-B).

4.2. Envelope response.

Figure 6 shows the load-displacement envelope curves of all the specimens. It should be noted that due to the similarity of the results obtained for each pair of specimens (0.5%-A and 0.5%-B; 1%-A and 1%-B; 1.5%-A and 1.5%-B; 1.5%SF-A and 1.5%SF-B), the results shown in Figure 6 shown the average for each pair of specimens. From load-displacement envelope response, the stiffness variations of each specimen can be obtained as the ratio between the load applied and displacement. The load-displacement envelope curves also show the load that cause the failure at the base of the column.

From these results it can be concluded:

- NF and RC specimens had lower loads than the loads supported by the UHPFRC specimens (0.5%, 1%, 1.5%, 2% and 1.5% SF), due to the lack of fibers. NF and RC specimens reached maximum loads of 17 and 15 kN for a drift ratio of 2% and 3%, respectively (displacements of 26 and 39 mm).
- The 2% specimen reached the greatest load with a value of 24 kN for a drift ratio of 2.5%. This value is 60% higher than the RC specimen and 41% higher than NF specimen.
- The use of fibers increases the maximum horizontal load by an average of 30% more than that of the NF and 48% more than the RC.
- All the specimens presented linear behavior during the first load cycles and up to a drift ratio of approximately 1.5%, which corresponds to a displacement close to 20 mm. From now on, more significant differences are observed depending on the fiber percentage of each specimen.
- The use of SF fibers (1.5% SF specimen) increases the specimens' initial strength but they cannot maintain the load with the same ductility as the others, as their maximum horizontal load degenerates at drift ratios over 2% (displacement of 26 mm). This is due to a greater loss of adherence in SF than in HK, which provide a high anchorage effect.
- 2% specimen suffers a sudden strength loss from a 4% drift ratio (displacement of 52mm). This behavior is observed only for one displacement direction and is due to the sudden cracking of the concrete that has not been properly tied by the fibers. As seen later, the 2% specimen showed deficient workability when being poured. From now on, strength remains constant with a ductile behavior until the end of the test.

- 0.5%, 1% and 1.5% specimens present a very similar behavior. From a 1.5% drift ratio (displacement of 20mm), the strength of the specimens remains constant with a high ductility, until reaching drift ratio of 6% (displacement of 78 mm). This behavior can be observed equally in both directions of displacement.
- The UHPFRC specimens had higher initial stiffness than the RC and NF specimens, as seen in the steeper slope of the initial linear part of the load-displacement envelope curve.

4.3. Energy dissipation capacity.

The energy dissipated in a single load cycle is obtained by using the trapezoid rule to determine the area within the vertical load versus the displacement of the corresponding drift ratio. The amount of cumulative energy dissipated by the specimens during the test (the average of three load cycles under the same displacement) is shown in Figure 7. It should be noted that due to the similarity of the results obtained for each pair of specimens (0.5%-A and 0.5%-B; 1%-A and 1%-B; 1.5%-A and 1.5%-B; 1.5%SF-A and 1.5%SF-B), Figure 7 shown the average for each pair of specimens.

In view of the results, the following can be stated:

- The amount of dissipated energy at the start of the test was similar in all the UHPFRC specimens. RC and NF specimens accumulated the least energy due to their not having fibers. Despite this, NF specimen dissipated 92% more energy than the RC specimen.
- After a displacement of approximately 25 mm (drift ratio close to 2%) the amount of energy dissipated by the specimens was seen to change, due to the cracks at the base of the columns and the contribution of the fibers, which helped to dissipate energy. In this way, the UHPFRC specimens showed better behaviour than the RC and NF specimens, since the fibers delayed cracking.
- 1.5% SF specimen dissipated less energy at high displacement values than 1.5% specimen, which was due to a greater loss of adherence in straight fiber (SF) than in hooked fiber (HF), which provide a high anchorage effect.
- 1% specimen dissipated less energy at high displacement values than 0.5% specimen, which can be considered abnormal and was due to a non-homogeneous distribution of the fibers inside the concrete, when it was being poured into the formwork. The authors consider that a problem in

the construction process was the cause, specifically, an excess of vibrating of the UHPFRC.
After the test all specimens were examined, the beam and the column were cut and separated,
and the fibers in the joint were located and quantified. In 1%-A and 1%-B specimens, fibers were seen to be concentrated in the centre of cross section (see Figure 8), but were found to be evenly distributed in 0.5%-A and 0.5%-B specimen, which allowed them to work better and thus dissipate higher amounts of energy.

- Something similar happened to the 2% specimen, which had a lower energy dissipation capacity than the 1.5% specimens, due to its deficient workability when being poured.
- At the end of the test, 1.5%, 1.5% SF, 1% and 0.5% specimens dissipated, on average, 216%, 186%, 157% and 179% more energy than the RC specimen, respectively. With respect NF specimen, 1.5%, 1.5% SF, 1% and 0.5% specimens dissipated 65%, 49%, 34% and 45% more energy than the NF specimen, respectively.
- The experimental results show that the performance of the 1.5% specimen was better than the others. It is important to point out that 1.5% steel fiber dosages allow the correct workability and pouring of the mixture.
- The great capacity of the UHPFRC specimens to dissipate energy shows that steel fibers improve the behavior of structural members subjected to cyclic loadings.

Figure 9 shows the average energy dissipated in each three load cycles under the same displacement. In view of the results, the following can be stated:

- In UHPFRC specimens, the energy dissipated by the cycles increases until a drift ratio of 5% (displacement of 65 mm). From this drift ratio degradation can be considered to start and is reflected because for higher drift ratio, the energy dissipated in each cycle practically does not increase, and even decreases as in the case of 1.5% and 2% specimens.
- The behavior of NF and RC specimens is quite similar, although the NF specimen dissipates a greater amount of energy in each cycle than the RC specimen. For this case, energy dissipated in each cycle increases until reaching a drift ratio of 4% corresponding to a displacement of 52mm. From now on, the energy dissipated by each cycle decreases, which indicates that the NF and RC specimens show greater degradation for lower drift values, with respect to the UHPFRC specimens.

4.4. Stiffness degradation

Stiffness was seen to degrade during the test (see Figure 10.a). Using the envelopes, the values of initial stiffness were calculated as the averages of the push and pull directions.

In view of these results the following can be stated:

- The stiffness of all the specimens is degraded with time during the tests due to the cracking at the base of the columns.
- Similar results were obtained for each pair of specimens (0.5%-A and 0.5%-B; 1%-A and 1%-B; 1.5%-A and 1.5%-B; 1.5%SF-A and 1.5%SF-B). The differences of stiffness variation between the two specimens of the same mix are negligible. For this reason, Figure 10 shown the average for each pair of specimens.
- The initial stiffness of the specimens varied between approximately 1.4 and 2.8 kN/mm, the stiffest being those with the highest dosage of fibers. The RC specimen was the least stiff. Fibers dosage has a higher influence on stiffness. For example, 1.5% specimen is 72% stiffer on average than the RC specimen.
- After the 3% drift ratio (displacement of 39 mm) the stiffness of all the specimens were quite similar and small, except for RC and NF specimens, which remained below the rest.
- However, it is important to highlight that the relationship between the initial and final stiffness of each specimen is quite similar. This means that the stiffness percentage losses with respect to the initial stiffness k_0 of each specimen is very similar for all the specimens (Figure 10.b). For a drift ratio of 6% (displacement of 78 mm), stiffness of all the specimens varies, on average, between 13% and 7.7% of its initial stiffness. These values correspond to the RC and 1.5%-SF specimens.
- All the specimens suffered the greatest loss of stiffness in the early stages of the test (Figure 10.b), specifically to a displacement of 6 mm (drift ratio of 0.5%). On average, up to a displacement of 6 mm, the UHPFRC specimens lost 45% of their initial stiffness, NF specimen lost 53 % of its initial stiffness and the RC specimen lost 52% of its initial stiffness. Once this drift ratio has been exceeded, the stiffness of all specimens decreases but with a lower slope.

4.5. Cracking pattern.

The cracking patterns were compared using photos of the bottom of the columns and the beam-columns joint of the different specimens. Figure 11 shows the evolution of the cracks in each specimen at different drift ratios of 1%, 2% and 3%. From these results it can be concluded:

- As the cycles progressed, the first bending and horizontal cracks were observed at bottom of the column, close to joint region.
- For UHPFRC, failure was in general due to the bending of the column, with horizontal cracks in the bottom section but with no serious damage at the joint. The even distribution of the fibers within the columns in UHPFRC specimens avoided the propagation of severe cracking. The first bending cracks were observed at the bottom of the column at an imposed displacement of close to 6 mm (drift ratio close to 0.5%). Cracks due to plastic settlement were noted in the 1.5% specimen before the test, which caused the crack to occur away from the joint over one of the stirrups. This effect had greater impact in this specimen due to the atmospheric conditions of the day of the pouring and curing the specimen. Specifically, that day there was a medium-low humidity and high temperatures, which caused more exudation.
- Of all UHPFRC specimens, 2% showed the least damage level at the end of the test. 0.5% specimen was the one that reached the highest damage level.
- However, in RC and NF specimens, the cracks at the bottom of the column caused degradation and loss of material and reduced the element's strength and the adherence of the rebars reinforcement.
- The RC and NF specimens highlighted also a significant vulnerability in the joint region, where there was also a typical shear failure (tilted cracking). The first signs of damage occurred at the column during an imposed displacement of 3.5 mm (close to 0.3% drift ratio). These cracks were small and flexural. For NF specimen, bending cracks were increasing at the bottom of the column until reaching a high level of damage when drift ratio was close to 1% (Figure 10). For RC specimens, these bending cracks did not reach as much spread as in the NF specimen.
- Several cracks then started to develop in the joint region, that affect the strength of the specimen when the cracks along the two diagonals of the joint became dominant (Figure 10). At the end of the test, it could be seen that the failure for NF and RC specimens was characterized by spalling of the concrete and considerable loss of material.

- The use of steel fibers greatly improved the columns' cyclic behaviour and avoided the spalling and loss of material seen in the NF and RC specimens.

4.6. Cracking area

The cracking area for each displacements were measured by digital images software taking into account the width and length of the cracks. The photographic acquisition system was configured to take a photograph (of each of the two sides of the beam-column joint) when the last maximum displacement was applied in each of the load cycles, both when the dynamic actuator was in tension and when it was under compression. Figure 12 show the values of the crack pattern area vs displacements applied to the upper part of the column.

It can be seen in Figure 12 that in general the UHPFRC specimens greatly restricted the cracking propagation since they have fewer cracking areas. In the RC and NF specimens the cracking areas tend to grow as the imposed displacement increases.

Here again it can be seen that RC and NF specimens suffer increased degradation as the imposed displacement rises, as they present large cracking areas. On average, for an displacement of 39 mm (3% drift ratio) the fibers have reduced the cracked area by between 40 and 62% compared to the NF specimen and between 15 and 43% compared to RC specimen.

5. Conclusions.

This paper describes a cyclic tests carried out on UHPFRC beam-column joints specimens. A total of 11 specimens were built with the same geometry and reinforcement, the only difference being in the percentage of fibers per concrete volume.

The dosages used in the experimental test were 0% (NF specimen), 0.5%, 1%, 1.5%, 2% for hooked fibers (HF) and 1.5% for straight fibers (SF). The specimen designs were based on NSR-10 with moderate energy dissipation capacity.

Considerable differences were observed between specimens with different fiber dosages and the following conclusions can be drawn:

- The great capacity of UHPFRC specimens with fibers to dissipate energy shows that steel fibers improve the behaviour of structural members subjected to cyclic loading. UHPFRC specimens have at least 157% higher energy dissipation than RC specimen.

- The maximum load reached by the UHPFRC specimens with fibers was 30 % higher on average than that of the NF specimen and 48% higher than that of the RC specimen.
- The experimental results show that the performance of the 1.5% specimen was better than the others and gave no workability or pouring problems. The reason for this is that the 2% specimen was difficult to work during pouring and this affected the quality of the specimen. It is therefore not recommended to use fiber dosages above 1.5%.
- The UHPFRC specimens have greater initial stiffness than the RC and NF. Fibers dosage has a higher influence on stiffness; for example, the stiffness of 1.5% specimen is 72 % higher than the RC specimen.
- The stiffness of all the specimens degraded as the tests advanced. On average, up to a displacement of 6 mm, the UHPFRC specimens lost 45% of their initial stiffness, NF specimen lost 53 % of their initial stiffness and the RC specimen lost 52% of its initial stiffness.
- The specimen with the lowest stiffness is the one with conventional concrete, RC, although it is important to point out that the percentage stiffness lost of all the specimens is quite similar.
- In general, the failure of the UHPFRC specimens is produced by column bending, which causes horizontal cracks at the bottom of the column. In this respect, the use of steel fibers greatly improves the column's cyclic behavior and avoids the severe cracking and loss of material that occurred in the case of the NF and RC specimens. However, the RC and NF specimens highlighted also a significant vulnerability in the joint region.

Acknowledgements

This work was supported by Cementos Argos, Colciencias and the Pontificia Universidad Javeriana, Bogotá (Colombia).

References.

- [1] Ruiz Pinilla JG. Estudio experimental de nudos interiores viga-columna de entramados de hormigón armado con detalles no-dúctiles, con columnas reforzadas mediante angulares y presillas de acero, sometidos a cargas cíclicas. Universitat Politècnica de València, 2013. doi:10.4995/Thesis/10251/33752.
- [2] Ruiz-Pinilla JG, Adam JM, Pérez-Cárcel R, Yuste J, Moragues JJ. Learning from RC building structures damaged by the earthquake in Lorca, Spain, in 2011. *Eng Fail Anal* 2016;68:76–86. doi:10.1016/j.engfailanal.2016.05.013.
- [3] Adam JM, Pallarés FJ. Editorial (Strengthening of structures under seismic loads). *Proc Inst Civ Eng - Struct Build* 2014;167:1. doi:10.1680/stbu.2013.167.1.1.
- [4] Adam JM, Pallares FJ. Editorial (Learning from Structural Failures). *Eng Struct* 2010;32:1791. doi:10.1016/j.engstruct.2010.04.026.
- [5] Adam J. Global research continues into strengthening structures against earthquakes. *Proc Inst Civ Eng - Civ Eng* 2015;168:148–148. doi:10.1680/cien.2015.168.4.148.
- [6] Adam J, Ingham J. Editorial (Structural Failures in Earthquakes). *Eng Fail Anal* 2013;34:536. doi:10.1016/j.engfailanal.2013.07.029.
- [7] Moehle JP, Mahin SA. Observations on the Behavior of Reinforced Concrete Buildings During Earthquakes. *Spec Publ n.d.*;127. doi:10.14359/3007.
- [8] Gillies AG, Anderson DL, Mitchell D, Tinawi R, Saatcioglu M, Gardner NJ, et al. The August 17, 1999, Kocaeli (Turkey) earthquake — lifelines and preparedness. *Can J Civ Eng* 2001;28:881–90. doi:10.1139/101-055.
- [9] Sezen H, Whittaker A., Elwood K., Mosalam K. Performance of reinforced concrete buildings during the August 17, 1999 Kocaeli, Turkey earthquake, and seismic design and construction practise in Turkey. *Eng Struct* 2003;25:103–14. doi:10.1016/S0141-0296(02)00121-9.
- [10] Doğangün A. Performance of reinforced concrete buildings during the May 1, 2003 Bingöl Earthquake in Turkey. *Eng Struct* 2004;26:841–56. doi:10.1016/j.engstruct.2004.02.005.
- [11] Ghobarah A, Saatcioglu M, Nistor I. The impact of the 26 December 2004 earthquake and tsunami on structures and infrastructure. *Eng Struct* 2006;28:312–26. doi:10.1016/j.engstruct.2005.09.028.
- [12] Arslan MH, Korkmaz HH. What is to be learned from damage and failure of reinforced concrete

- structures during recent earthquakes in Turkey? *Eng Fail Anal* 2007;14:1–22. doi:10.1016/j.engfailanal.2006.01.003.
- [13] Kim SJ, Elnashai AS. Characterization of shaking intensity distribution and seismic assessment of RC buildings for the Kashmir (Pakistan) earthquake of October 2005. *Eng Struct* 2009;31:2998–3015. doi:10.1016/j.engstruct.2009.08.001.
- [14] Lee J-Y, Kim J-Y, Oh G-J. Strength deterioration of reinforced concrete beam–column joints subjected to cyclic loading. *Eng Struct* 2009;31:2070–85. doi:10.1016/j.engstruct.2009.03.009.
- [15] ACI Committee 318. Building code requirements for structural concrete (ACI 318-14). Detroit: 2014.
- [16] Calavera Ruiz J. Patología de estructuras de hormigón armado y pretensado. Madrid: INTEMAC; 2005.
- [17] Ruiz-Pinilla JG, Pallarés FJ, Gimenez E, Calderón PA. Experimental tests on retrofitted RC beam-column joints underdesigned to seismic loads. General approach. *Eng Struct* 2014;59:702–14. doi:10.1016/j.engstruct.2013.11.008.
- [18] Abbas AA, Syed Mohsin SM, Cotsovos DM. Seismic response of steel fiber reinforced concrete beam–column joints. *Eng Struct* 2014;59:261–83. doi:10.1016/j.engstruct.2013.10.046.
- [19] Realfonzo R, Napoli A, Ruiz-Pinilla JG. Cyclic behavior of RC beam-column joints strengthened with FRP systems. *Constr Build Mater* 2014;54:282–97. doi:10.1016/j.conbuildmat.2013.12.043.
- [20] Akguzel U, Pampanin S. Assessment and Design Procedure for the Seismic Retrofit of Reinforced Concrete Beam-Column Joints using FRP Composite Materials. *J Compos Constr* 2012;16:21–34. doi:10.1061/(ASCE)CC.1943-5614.0000242.
- [21] Au FTK, Huang K, Pam HJ. Diagonally-reinforced beam–column joints reinforced under cyclic loading. *Proc Inst Civ Eng - Struct Build* 2005;158:21–40. doi:10.1680/stbu.2005.158.1.21.
- [22] Fukuyama H, Sugano S. Japanese seismic rehabilitation of concrete buildings after the Hyogoken-Nanbu Earthquake. *Cem Concr Compos* 2000;22:59–79. doi:10.1016/S0958-9465(99)00042-6.
- [23] Li B, Chua HYG. Seismic Performance of Strengthened Reinforced Concrete Beam-Column Joints Using FRP Composites. *J Struct Eng* 2009;135:1177–90. doi:10.1061/(ASCE)0733-9445(2009)135:10(1177).
- [24] Ghasemi S, Zohrevand P, Mirmiran A, Xiao Y, Mackie K. A super lightweight UHPFRC-HSS

- deck panel for movable bridges. *Eng Struct* 2016;113:186–93. doi:10.1016/j.engstruct.2016.01.046.
- [25] Habel K, Viviani M, Denarié E, Brühwiler E. Development of the mechanical properties of an Ultra-High Performance Fiber Reinforced Concrete (UHPFRC). *Cem Concr Res* 2006;36:1362–70. doi:10.1016/j.cemconres.2006.03.009.
- [26] Graybeal BA. Compressive Behavior of Ultra-High-Performance Fiber-Reinforced Concrete. *ACI Mater J* 2007;104:146–52. doi:10.14359/18577.
- [27] Graybeal BA. Structural Behavior of Ultra-High Performance Concrete Prestressed I-Girders. McLean, VA: 2006.
- [28] Graybeal BA. Characterization of the Behavior of Ultra-High Performance Concrete. University of Maryland, 2005.
- [29] Ahlborn TM, Peuse EJ, Misson DL. Ultra-High-Performance-Concrete for Michigan Bridges Material Performance – Phase I. Lansing, MI: 2008.
- [30] Spyridon A. Paschalis, Andreas P. Lampropoulos. Ultra-High-Performance Fiber-Reinforced Concrete under Cyclic Loading *ACI Materials Journal*, V. 113, No. 4, July-August 2016
- [31] Palacios G. Performance of full-scale ultra-high performance fiber-reinforced concrete column subjected to extreme earthquake-type loading and effect of surface preparation on the cohesion and friction factors of the AASHTO interface shear equation. University of Texas at Arlington, 2015.
- [32] Güvensoy G, Bayramov F, Ilki A, Sengül C, Tasdemir MA, Kocatürk N, et al. Mechanical Behavior of High Performance Steel Fiber Reinforced Cementitious Composites under Cyclic Loading Condition. In: M. Schmidt, E. Fehling CG, University of Kassel G, editors. *Proc. Int. Symp. Ultra High Perform. Concr., Kassel (Germany): 2004*, p. 649–60.
- [33] Bornemann R, Faber S. UHPC with steel- and non-corroding high-strength polymer fibers under static and cyclic loading. *Proc. Int. Symp. Ultra High Perform. Concr., Kassel (Germany): 2004*, p. 673–81.
- [34] Hung C-C, Yen W-M, Yu K-H. Vulnerability and improvement of reinforced ECC flexural members under displacement reversals: Experimental investigation and computational analysis. *Constr Build Mater* 2016;107:287–98. doi:10.1016/j.conbuildmat.2016.01.019.
- [35] Hung C-C, Su Y-F. On modeling coupling beams incorporating strain-hardening cement-based

- composites. *Comput Concr* 2013;12:565–83. doi:10.12989/cac.2013.12.4.565.
- [36] Canbolat A, Parra-Montesinos GJ, Wight JK. Experimental Study on Seismic Behavior of High-Performance Fiber-Reinforced Cement Composite Coupling Beams. *ACI Struct J* 2005;102:159–66. doi:10.14359/13541.
- [37] Hung C-C, Su Y-F, Yu K-H. Modeling the shear hysteretic response for high performance fiber reinforced cementitious composites. *Constr Build Mater* 2013;41:37–48. doi:10.1016/j.conbuildmat.2012.12.010.
- [38] Hung C-C, El-Tawil S. Seismic Behavior of a Coupled Wall System with HPFRC Materials in Critical Regions. *J Struct Eng* 2011;137:1499–507. doi:10.1061/(ASCE)ST.1943-541X.0000393.
- [39] Lequesne RD, Setkit M, Parra-Montesinos GJ, Wight JK. Seismic Detailing and Behavior of Coupling Beams With High-Performance Fiber Reinforced Concrete. In: American Concrete Institute, editor. *Symp. Four Decad. Prog. Prestress. Concr. , Fiber Reinf. Concr. Thin Laminate Compos. , SP - 272*, Farmington Hills, MI: 2010, p. 205–22.
- [40] Hung C-C, Chen Y-S. Innovative ECC jacketing for retrofitting shear-deficient RC members. *Constr Build Mater* 2016;111:408–18. doi:10.1016/j.conbuildmat.2016.02.077.
- [41] Weiqing Zhu, Jinqing Jia, Juncheng Gao, Fasheng Zhang. Experimental study on steel reinforced high-strength concrete columns under cyclic lateral force and constant axial load. *Engineering Structures* 125 (2016) 191–204.
- [42] Milad Mohammadi Hosinie, Hassan Aoude, William D. Cook, Denis Mitchell. Behavior of ultra-high performance fiber reinforced concrete columns under pure axial loading. *Engineering Structures* 99 (2015) 388–401
- [43] Hyun-Oh Shin, Kyung-Hwan Min, Denis Mitchell. Uniaxial behavior of circular ultra-high-performance fiber-reinforced concrete columns confined by spiral reinforcement. *Construction and Building Materials* 168 (2018) 379–393.
- [44] Hyun-Oh Shin, Kyung-Hwan Min, Denis Mitchell. Confinement of ultra-high-performance fiber reinforced concrete columns. *Composite Structures* 176 (2017) 124–142.
- [45] Shih-Ho Chao, Venkatesh Kaka, Guillermo Palacios, Jinsup Kim, Young-Jae Choi, Parham Aghdasi, Alireza Nojavan, Glen Allen, VA, Arturo Schultz. Seismic Behavior of Ultra-High-Performance Fiber-Reinforced Concrete Moment Frame Members. *First International Interactive Symposium on UHPC – 2016*.

Figure Captions

Figure 1. Geometry of the specimens. Dimensions in mm.

Figure 2. Sinusoidal displacements applied in the upper part of the columns.

Figure 3. Set-up of the cyclic load test.

Figure 4. Monotonic bending test on UHPFRC specimens.

Figure 5. Hysteretic load-displacement response for specimens: (a) 0.5%-A; (b) 0.5%-B; (c) 1%-A; (d) 1%-B; (e) 1.5%-A; (f) 1.5%-B; (g) 1.5%SF-A; (h) 1.5%SF-B; (i) 2%; (j) NF; and (k) RC.

Figure 6. Load-displacement envelope curves

Figure 7. Cumulative energy dissipation - Displacement

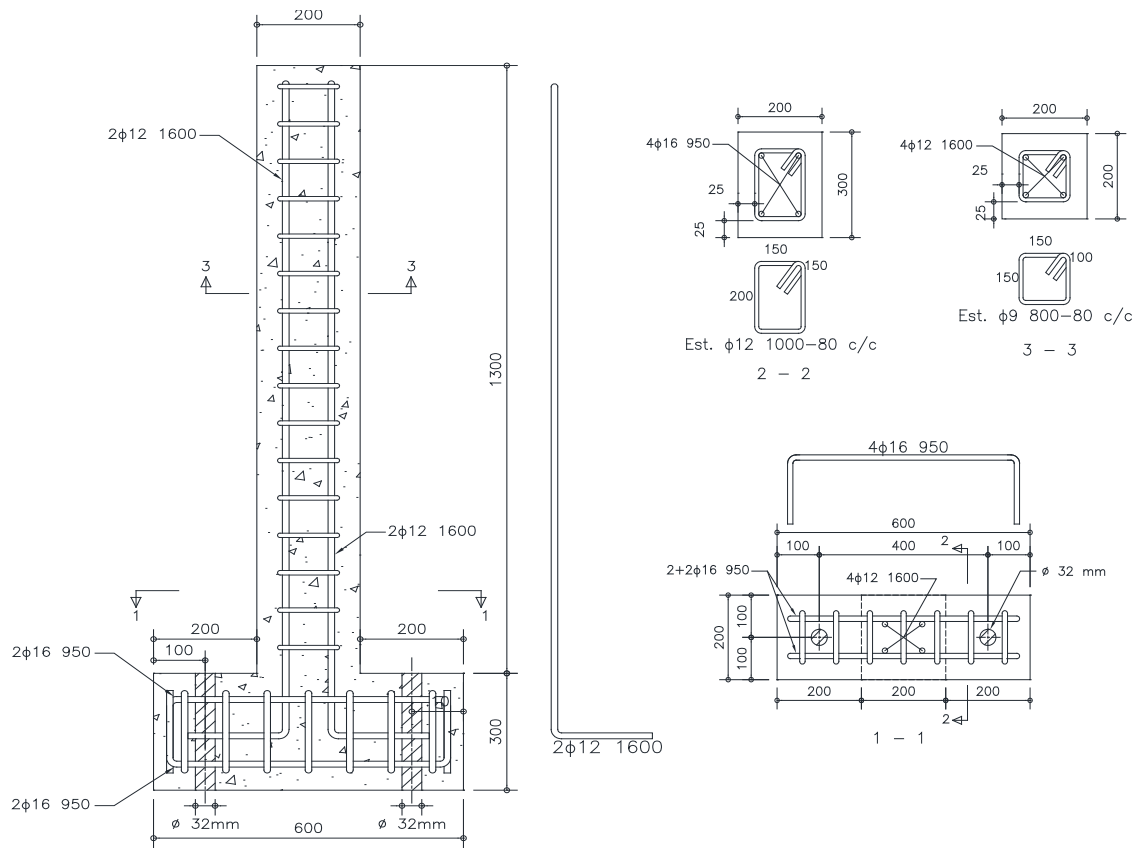
Figure 8. Non-homogeneous distribution of the fibers. In 1% specimens, fibers were concentrated in the centre of cross section. Red arrows show the load direction.

Figure 9. Energy dissipation in each cycle - Displacement

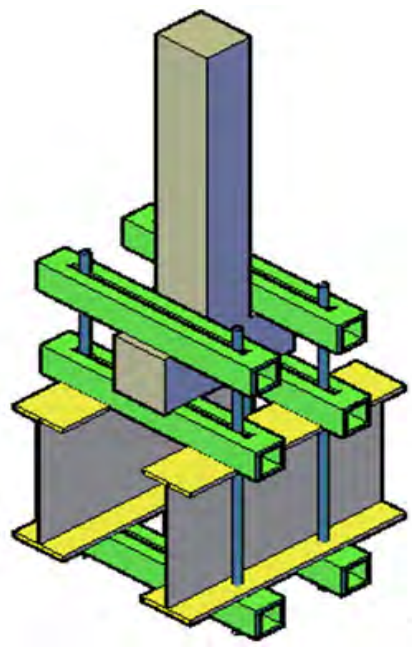
Figure 10. (a)- Stiffness degradation. (b)- Relative stiffness K/K_0

Figure 11. Evolution of the damage (cracking) in the specimens for different drift ratio.

Figure 12. Crack pattern area



(a)



(b)

Figura 1. Geometry of the specimens. Dimensions in mm.

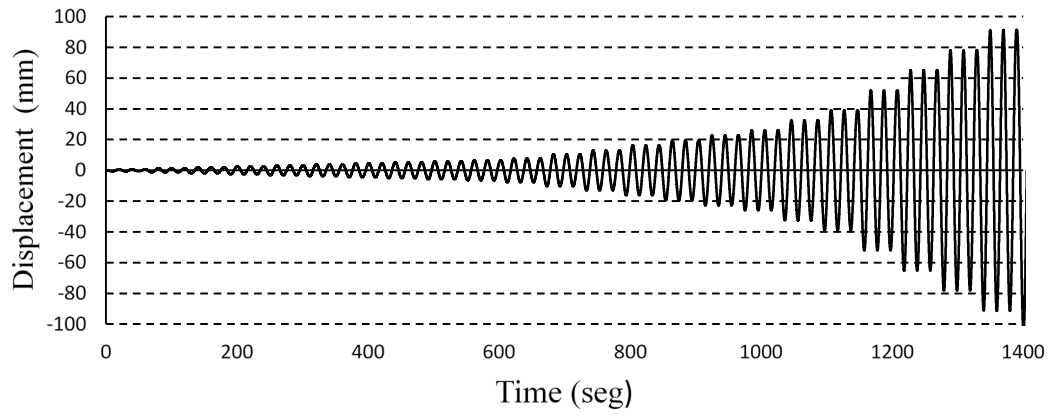


Figure 2. Sinusoidal displacements applied in the upper part of the columns.



Figure 3. Set-up of the cyclic load test.

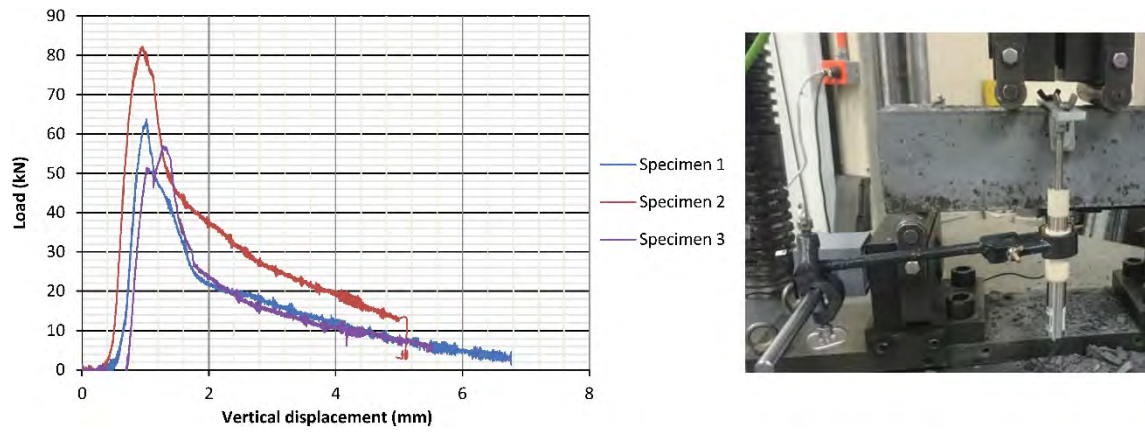
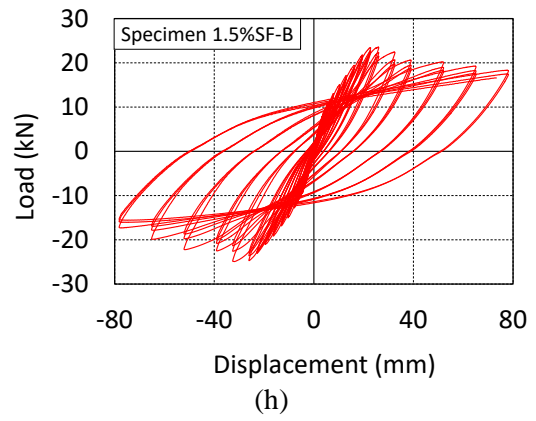
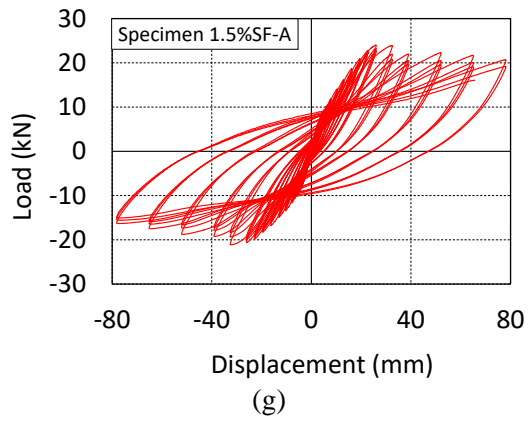
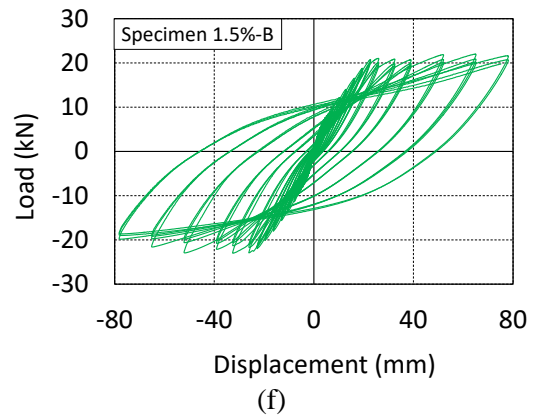
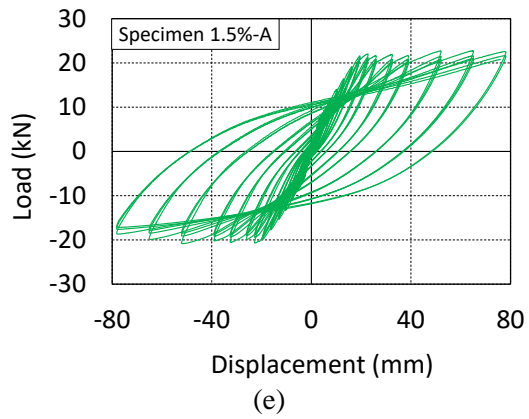
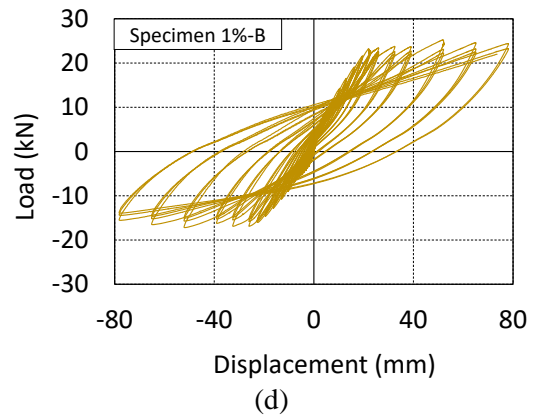
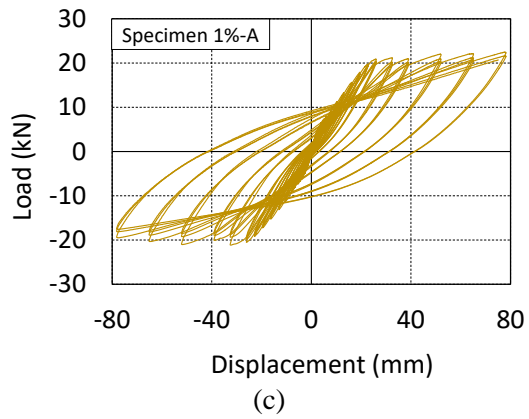
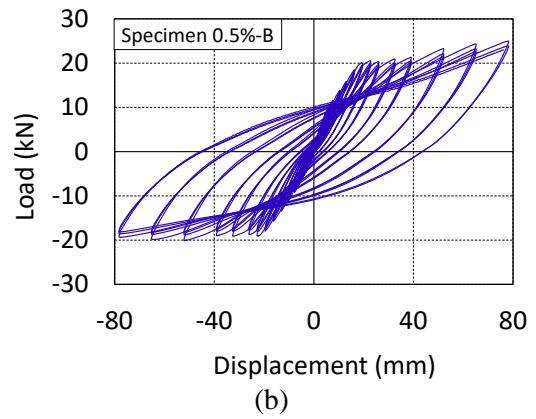
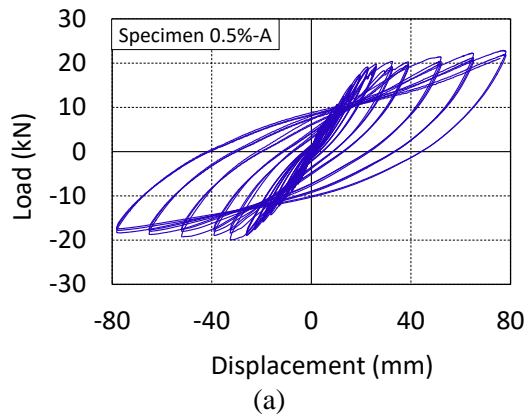
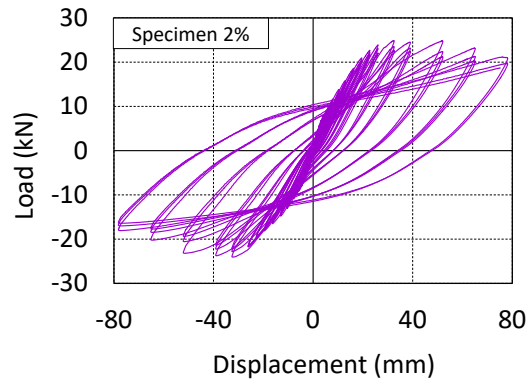
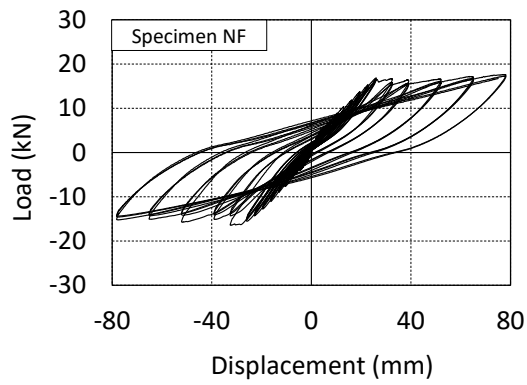


FIGURE 4 Monotonic bending test on UHPFRC specimens

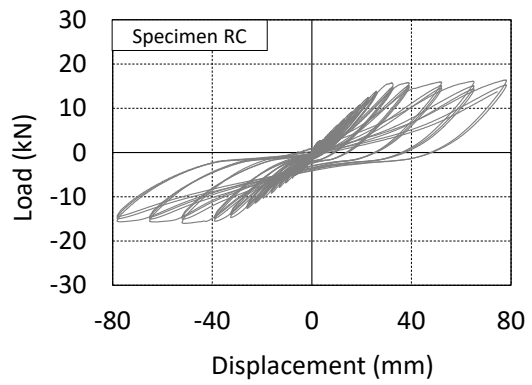




(i)



(j)



(k)

Figure 5. Hysteretic load-displacement response for specimens: (a) 0.5%-A; (b) 0.5%-B; (c) 1%-A; (d) 1%-B; (e) 1.5%-A; (f) 1.5%-B; (g) 1.5%SF-A; (h) 1.5%SF-B; (i) 2%; (j) NF; and (k) RC.

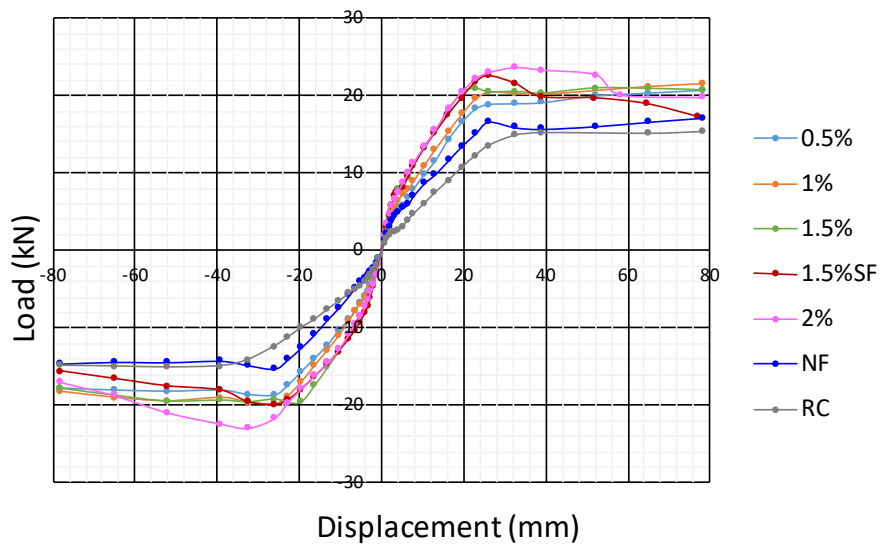


Figure 6. Load-displacement envelope curves.

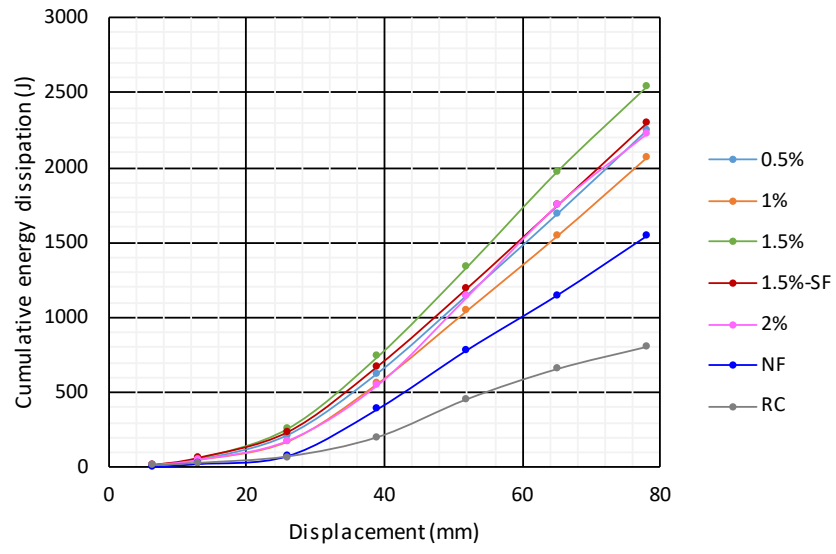


Figure 7. Cumulative energy dissipation - Displacement

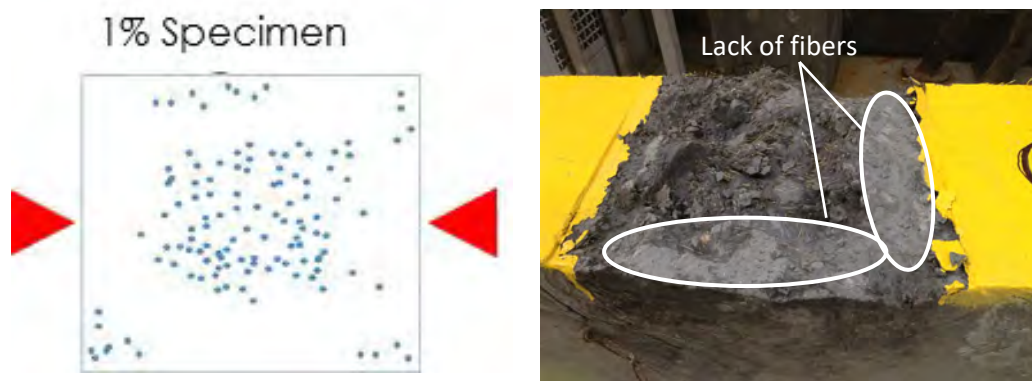


Figure 8. Non-homogeneous distribution of the fibers. In 1% specimens, fibers were concentrated in the centre of cross section. Red arrows show the load direction.

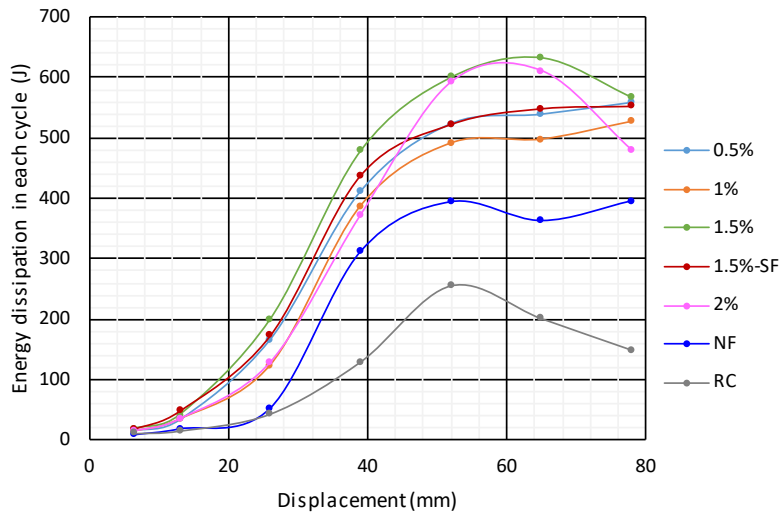
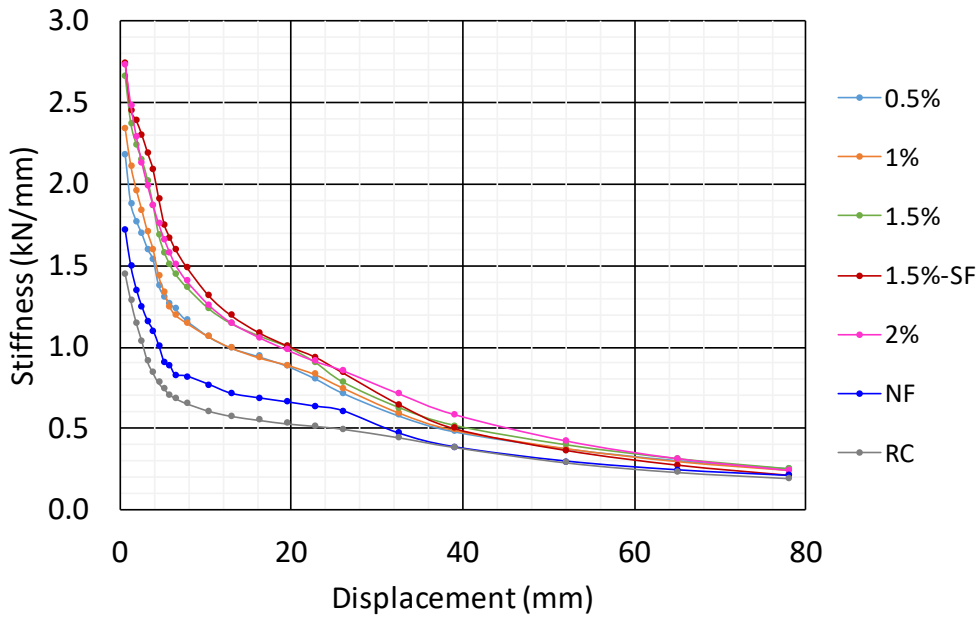
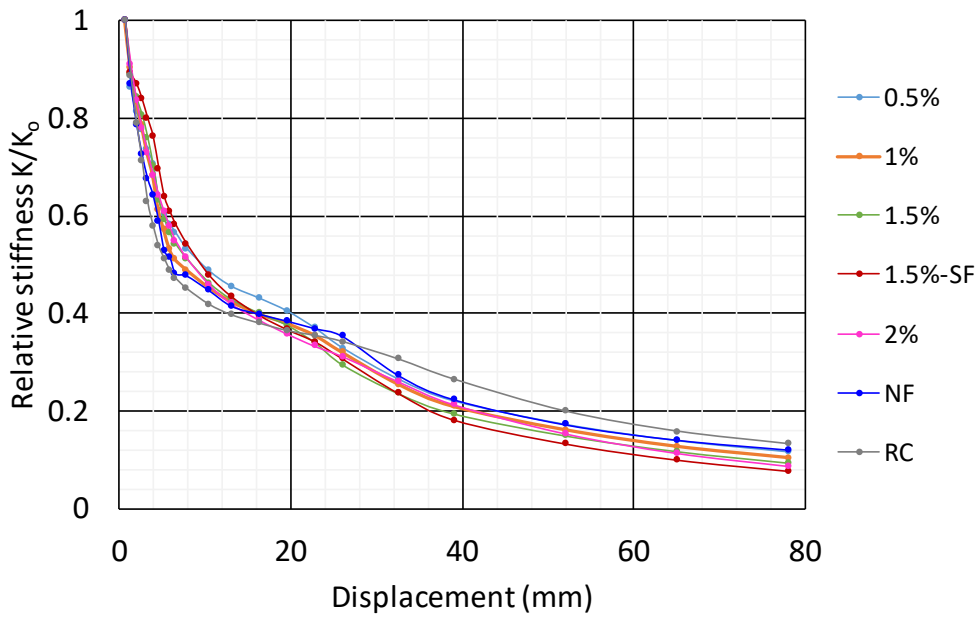


Figure 9. Energy dissipation in each cycle - Displacement

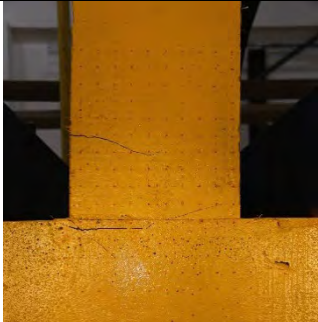
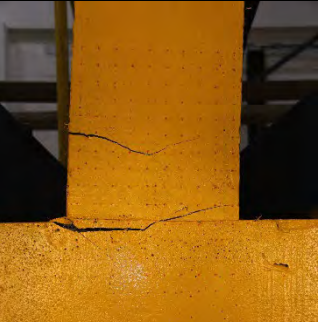

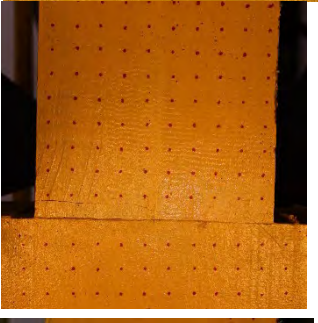
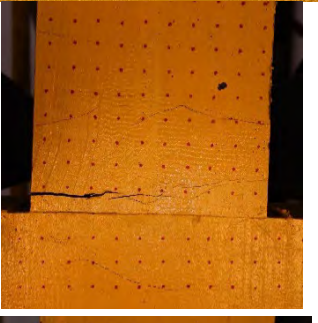
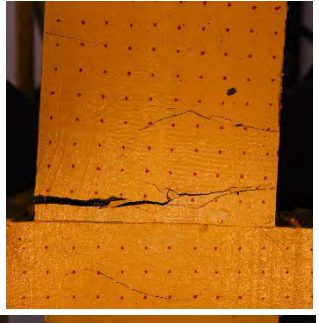
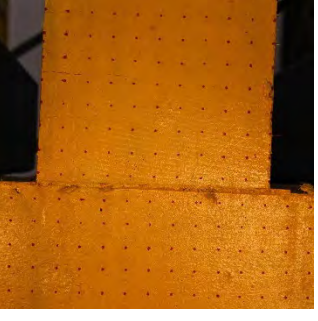

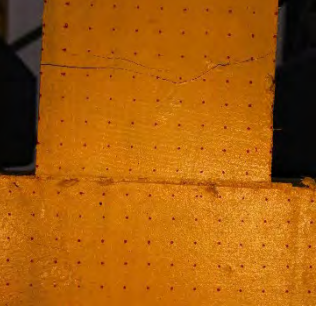
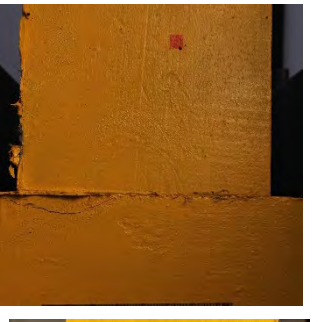
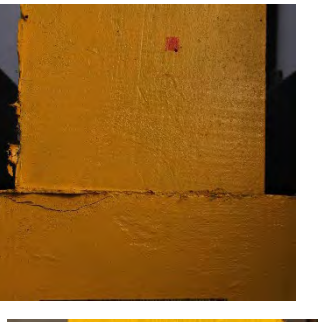
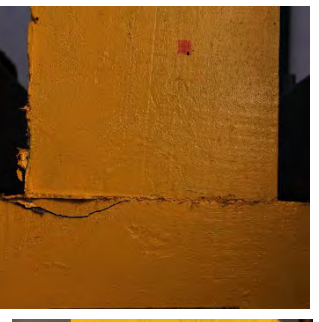
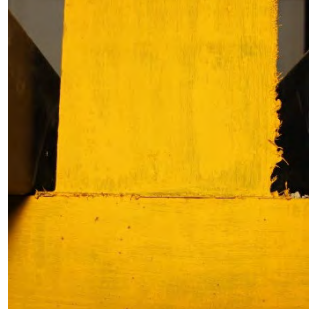
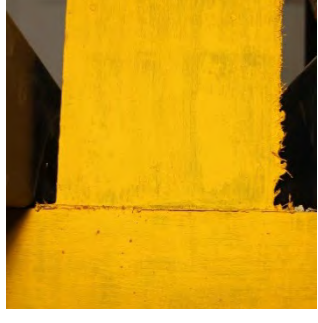
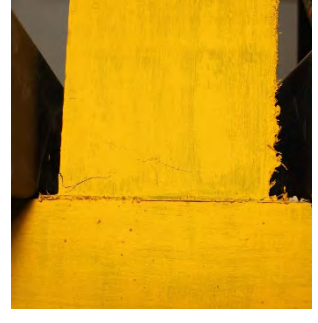


(a)



(b)

Figure 10. (a)- Stiffness degradation. (b)- Relative stiffness K/K_0

Drift Ratio			
Specimen	1%	2%	3%
0.5%			
1%			
1.5%			
1.5%SF			
2%			

NF



RC



Figure 11. Evolution of the damage (cracking) in the specimens for different drift ratio.

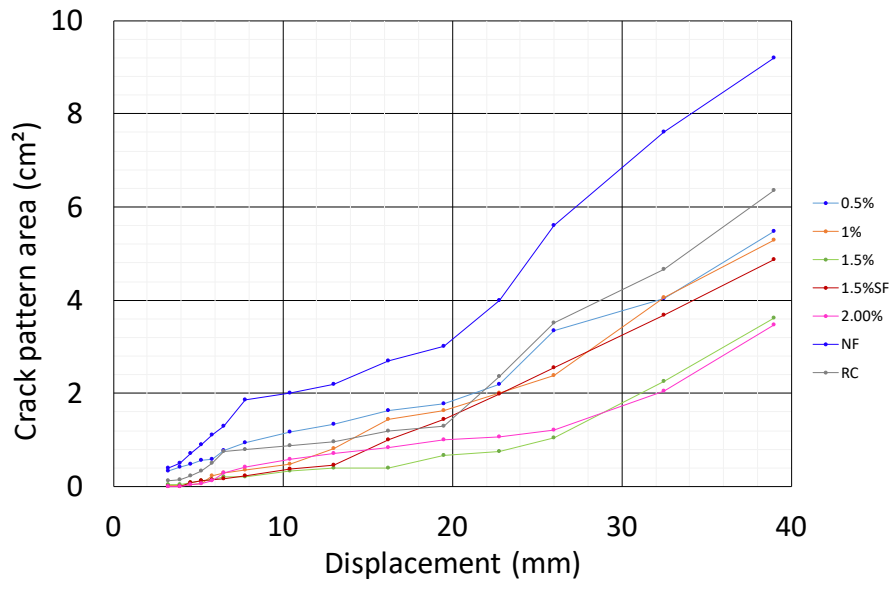


Figure 12. Crack pattern area